

<Original>

## The Transient Temperature Distribution in A Fluid-to-Solid System\*

Hyo Kyung Kim\*\*, Taik Sik Lee\*\*, Sung Tack Ro\*\* and Suk Hyun Kim\*\*\*

(Received Nov. 10, 1977)

유체-고체열교환계내에서의 비정상온도분포

김효경 · 이택식 · 노승탁 · 김석현

요 약

길이방향의 열전도효과가 비교적 큰 유체-고체 열교환계내에 일정한 높은 온도를 가진 유체가 유입될 때 이에 따른 비정상 온도분포가 해석되었다. 이러한 계를 기술하는 연립편미분 방정식의 수치해가 유한차분법에 의해 구해졌으며, 열전도가 무시된 경우에 대한 해석적 해를 구하여 위의 결과를 검증하였다. 한편 이상화된 모델에 대한 실험을 행하고 이 결과를 앞서 구한 수치해와 비교 검토하였다.

여기서 구해진 온도분포를 이용하여 축열효율  $\eta_A$  및  $\eta_B$ 를  $\eta_A$ 는 시간  $t$ 에서의 축열량과 정상상태에 도달했을 때의 축열량의 비로, 그리고  $\eta_B$ 는 시간  $t$ 동안의 축열된 양과 공급된 열량의 비로 정의하여

### Nomenclature

<b>English Letter Symbols</b>	
$A$ : total heat transfer area ( $m^2$ )	$V$ : volume ( $m^3$ )
$a$ : $hA/(\rho C_p V)f$ (1/sec)	$x$ : distance measured for inlet (m)
$b$ : $hA/(\rho C_p V)s$ (1/sec)	$z$ : dummy variables used in Eqs. (16) and (17)
$c_p$ : specific heat at constant pressure (J/kmK)	<b>Greek Letter Symbols</b>
$D, d$ : outer and inner diameter of the heat storage medium (m)	$\alpha$ : thermal diffusivity ( $m^2/sec$ )
$h$ : heat transfer coefficient ( $J/m^2sec K$ )	$\beta$ : $\alpha \cdot \frac{a^2}{b \cdot u^2}$ , dimensionless thermal diffusivity
$k$ : thermal conductivity ( $J/m sec K$ )	$\epsilon$ : void fraction of the packing
$L$ : length of heat storage medium (m)	$\eta$ : efficiency
$Q$ : quantity of stored heat (J)	$\theta$ : $\frac{T_s - T_0}{T_i - T_0}$ , dimensionless solid temperature
$S$ : cross sectiona area ( $m^2$ )	$\nu$ : $\frac{T_f - T_0}{T_i - T_0}$ , dimensionless fluid temperature
$T$ : temperature	$\xi$ : $\frac{x \cdot a}{u}$ , dimensionless distance from fluid-entry
$t$ : time (sec)	$\rho$ : density ( $kg/m^3$ )
$u$ : flow velocity of the fluid (m/sec)	$\tau$ : $(t - \frac{x}{u}) \cdot b$ , dimensionless time

### Subscripts

<p>*Presented at the KSME Conference, Taeku, May, 1977.</p> <p>**Member, Seoul National University</p> <p>***Member, Ulsan Institute of Technology</p> <p>Discussions on this paper should be addressed to the Editorial Department, KSME, and will be accepted until Februbry 15, 1978.</p>	<p><math>f</math> : working fluid</p> <p><math>i</math> : inlet</p> <p><math>m</math> : location node</p> <p><math>n</math> : time node</p> <p><math>o</math> : initial</p> <p><math>s</math> : solid (heat storage meidum)</p>
--	---

온도분포와 효율들에 대하여 시간변수  $\tau$ , 위치변수  $\xi$ 와 무차원 열확산율  $\beta$ 가 미치는 영향을 조사하였다. 이에 따르면 온도는  $\beta$ 가 적어짐에 따라 점점 가파르게 분포되고 한편  $\eta_A$ 는  $\tau$ 가 점점 커지거나,  $\xi$ 가 작아질수록 좋아지는 것을 알 수 있다. 또한  $\eta_B$ 는  $\eta_A$ 와는 정반대의 경향을 보여 주어 축열제의 최적상태가 존재함을 알 수 있다.

### 1. INTRODUCTION

In connection with the lack of fuel resources, many investigations have been made to develop new energy resources or to utilize the conventional thermal energy more efficiently. Among the studies, heat storage problem becomes one of the important subjects to be solved.

For example, in solar heating system, the storage of solar energy is required to provide heat for the night and cloudy days. And heat storage is also needed to utilize electric power during its off-peaktime. Practically, in the last some years, there has been a considerable growth of interest in the possibility of providing some of the energy requirement of buildings by direct collection of solar energy.

There have been a number of heat transfer studies for the heat storage system by Nusselt, Hausen, and Schumann.<sup>1)</sup> However, most of the previous work did not consider the effect of heat conduction along axial direction. In addition, most of the experimental investigations of this problem did not include the effect of axial conduction by using spheres or granulate particles as heat storage medium<sup>2-5)</sup>.

In this work, the transient temperature distributions in fluid-to-solid heat exchanger system with axial conduction are studied, so that the results may be applied to direct contact, specific-heat type storage unit.

This type unit accumulates the heat ener-

gy obtained from working fluid in the heat storage medium of large heat capacity. When the medium is continuous along the longitudinal direction and/or has relatively high thermal conductivity, the effect of axial conduction in the solid phase can not be neglected anymore.

### 2. ANALYSIS

#### 2.1. Governing Equation

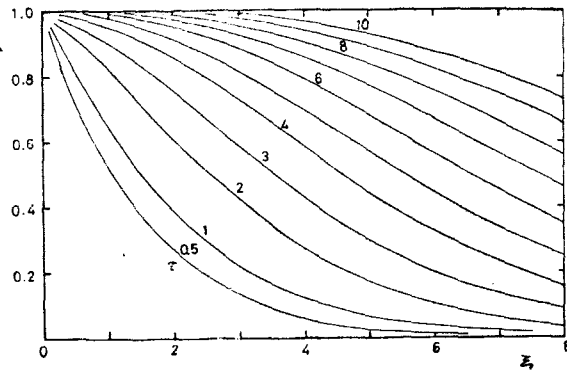


Fig. 1. Idealized heat storage system

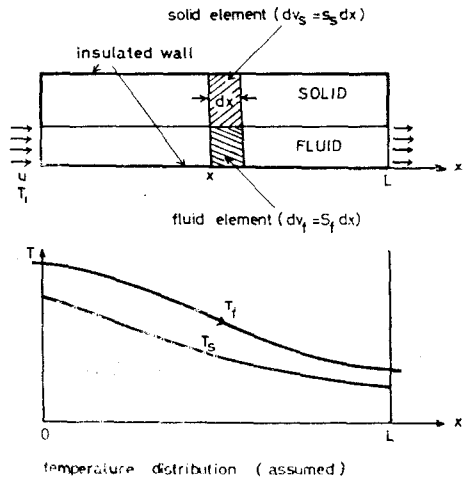


Fig. 2. Dimensionless fluid temperature for  $\beta=0$

The physical system discussed in this paper is shown in Fig. 1. The hot fluid at temperature,  $T_i$ , flows through the fluid passage of the system which was initially at temperature,  $T_0$ .

The heat transfer process in the system consists of forced convection between the fluid and the solid, and axial conduction in the solid phase.

The partial differential equations for the performance of the system can be given with the following assumptions.

(1) Heat conduction in the solid medium and fluid flow are one dimensional in a direction normal to the bounding surface.

(2) The system has constant thermo-physical properties.

(3) Heat conduction within the fluid is negligible.

(4) No heat losses to the environment occur.

Then heat balance may be described on the fluid contained in elemental slice of the system,  $dV_f$ , in Fig. 1 as,

$$\frac{\partial T_f}{\partial t} + a(T_f - T_s) + u \frac{\partial T_f}{\partial x} = 0 \quad (1)$$

where

$$a = \frac{h \cdot A}{(\rho C_p V)_f}$$

A similar heat balance on the solid element,  $dV_s$ , can be given as,

$$\frac{\partial T_s}{\partial t} + b(T_s - T_f) - \alpha \frac{\partial^2 T_s}{\partial x^2} = 0 \quad (2)$$

where

$$b = \frac{h \cdot A}{(\rho C_p V)_s}, \quad \alpha = \frac{k}{(\rho C_p)_s}$$

The appropriate initial and boundary conditions for the Eqs. (1) and (2) are

$$T_f(x, 0) = T_s(x, 0) = T_0, \quad (3)$$

$$T_f(x, t) = T_i, \quad (4)$$

$$\frac{\partial T_s}{\partial x} = 0 \text{ at } x=0, L. \quad (5)$$

## 2.2. Non-dimensionalization

For further application to general situations, Eqs. (1) and (2) are normalized and nondimensionalized.

It is natural to introduce dimensionless temperatures  $\nu = \frac{T_f - T_0}{T_i - T_0}$  and  $\theta = \frac{T_s - T_0}{T_i - T_0}$  for fluid and solid temperature respectively. In order to nondimensionalize the independent variables, some characteristic and reference quantities are determined. First, the quantity,  $t_c = \frac{x}{u}$ , is considered as a kind of characteristic time of the system because it describes the affected time of fluid due to the system (i.e. the time duration of the fluid flow from inlet to location,  $x$ ). On the other hand, simpler substitutes,  $a$

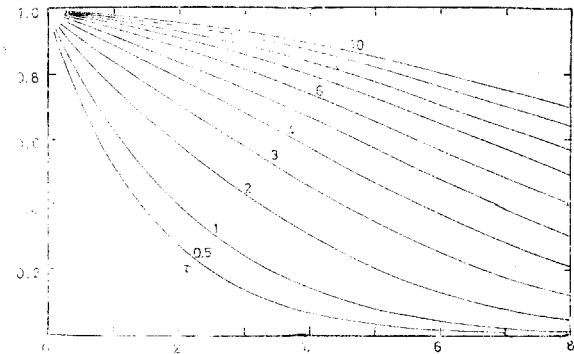


Fig. 3. Dimensionless fluid temperature for  $\beta=1$

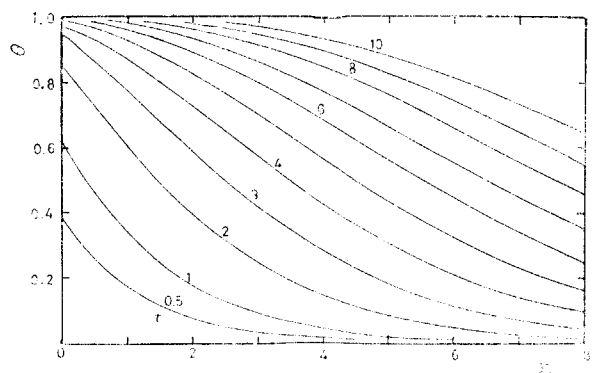


Fig. 4. Dimensionless solid temperature for  $\beta=0$

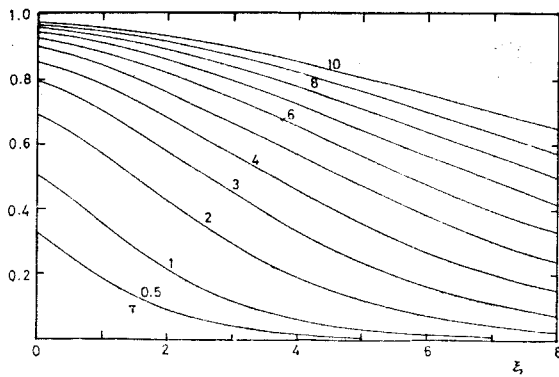


Fig. 5. Dimensionless solid temperature for  $\beta=1$ .

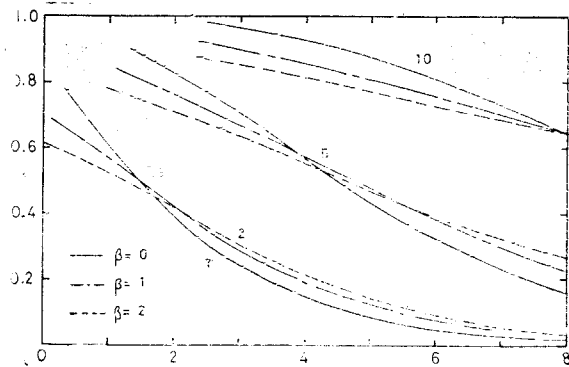


Fig. 7. Effect of  $\beta$  on solid temperature.

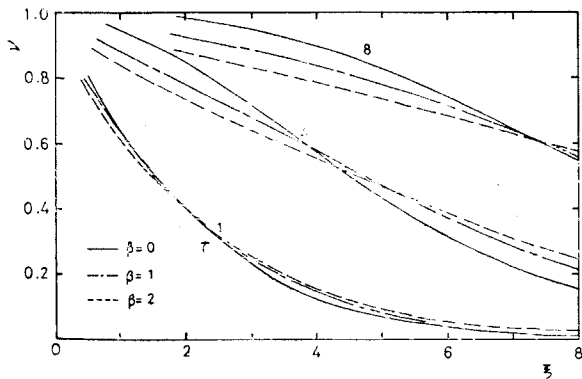


Fig. 6. Effect of  $\beta$  on gas temperature.

and  $b$ , are examined as important parameters because they have the dimension of a reciprocal of time. We define the dimensionless time variable as  $\tau = \left(t - \frac{x}{u}\right) \cdot b$  and dimensionless location variable as  $\xi = \frac{a \cdot x}{u}$ .

By using these variables, the governing equations with initial and boundary conditions can be ultimately written as

$$\frac{\partial \nu}{\partial \xi} + (\nu - \theta) = 0 \tag{6}$$

$$\frac{\partial \theta}{\partial \tau} + (\theta - \nu) - \beta \frac{\partial^2 \theta}{\partial \xi^2} = 0 \tag{7}$$

$$\theta(\xi, 0) = 0 \tag{8}$$

$$\nu(0, \tau) = 1 \tag{9}$$

$$\frac{\partial \theta}{\partial \xi} = 0 \text{ at } \xi = 0, \quad \frac{a \cdot L}{u} \tag{10}$$

where

$$\beta = \frac{\alpha \cdot a^2}{b \cdot u^2}$$

Here, the dimensionless parameter,  $\beta$ , is recognized as the dimensionless thermal diffusivity.

### 2.3. The solution of the Governing Equation

The solution of the governing equations described in the previous section is obtained by means of standard finite difference technique<sup>6, 7</sup>. The final results are given by the solution of simultaneous equations which can be obtained easily by the standard Gauss-Jordan method.

The results are shown in Figs. 2–5 in which nondimensional temperatures  $\nu$  and  $\theta$  are given as a function of distance  $\xi$  for various time. Effects of thermal conduction  $\beta$  on the temperature distributions are presented in Figs. 6 and 7. It is evident from the figures that the conduction effect of the storage medium decreases the temperatures of fluid and solid in the entrance region. The opposite phenomena are shown in the downstream.

### 2.4. Energy Storage Efficiency

The following quantities are defined in relation to energy storage.

$$Q_c = S_s \cdot L \cdot (\rho C_p)_s \cdot (T_i - T_0) \quad (11)$$

$$Q_i = u \cdot S_f \cdot t \cdot (\rho C_p)_f \cdot (T_i - T_0) \quad (12)$$

$$Q_s = \int_0^L S_s \cdot dx \cdot (\rho C_p)_s \cdot (T_s - T_0) \quad (13)$$

where

$Q_c$ : the maximum heat capacity of storage medium

$Q_i$ : the heat supplied to the system during time  $t$

$Q_s$ : the stored energy in storage system during time  $t$ .

Using these quantities, two kinds of efficiencies,  $\eta_A$  and  $\eta_B$ , are defined, that is,

$$\eta_A = \frac{Q_s}{Q_c} \quad \text{and} \quad \eta_B = \frac{Q_s}{Q_i}$$

Here the efficiency,  $\eta_A$ , represents the ratio of the quantity of the energy stored at time  $t$  to the possible maximum of heat as  $t \rightarrow \infty$ . Another efficiency,  $\eta_B$ , means the ratio of the energy stored in the system to the quantity of the heat supplied at the inlet.

Then, by substituting  $Q_c$ ,  $Q_i$  and  $Q_s$  into defined efficiencies, we have,

$$\eta_A = \frac{\int_0^L (\rho C_p)_s \cdot S_s \cdot (T_s - T_0) dx}{(\rho C_p)_s \cdot S_s \cdot L \cdot (T_i - T_0)} = \frac{\int_0^{\xi_L} \theta d\xi}{\xi_L} \quad (14)$$

$$\eta_B = \frac{\int_0^L (\rho C_p)_s \cdot S_s \cdot (T_s - T_0) dx}{u \cdot S_f \cdot t \cdot (\rho C_p)_f \cdot (T_i - T_0)} = \frac{\int_0^{\eta_L} \theta d\xi}{\tau} \quad (15)$$

And these may be calculated by using the temperature distribution obtained in previous section.

The results of these and effects of  $\tau$ ,  $\xi$ , and  $\beta$  on these efficiencies are presented in Figs. 8-11.

### 3. EXPERIMENT

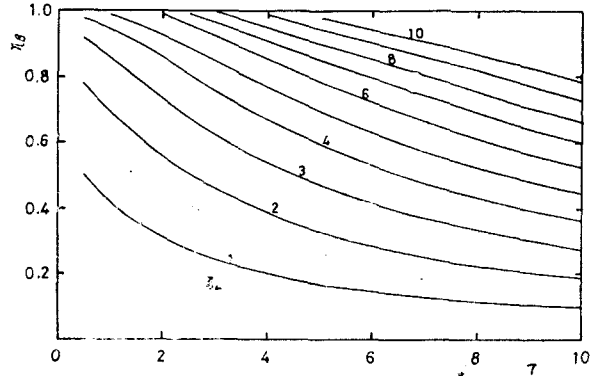


Fig. 8. Efficiency  $\eta_A$  vs. dimensionless time for  $\beta=1$ .

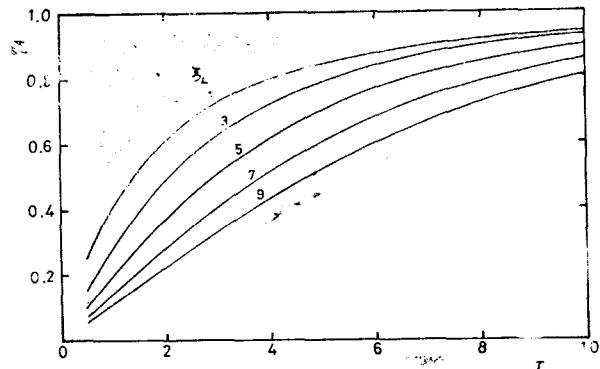


Fig. 9. Efficiency  $\eta_B$  vs. dimensionless time for  $\beta=1$ .

As discussed in introduction, one of the purpose of this work is to find the effects of the axial conduction. Therefore, the storage medium was taken to have high thermal conductivity, while air is used as transfer fluid. For the convenience of calculation and experiment, a hollow cylinder was chosen to be a geometry of the storage medium so that hot fluid may flow inside the cylinder.

The procedure to obtain the temperature distribution is described as follows.

The system initially at a uniform tem-

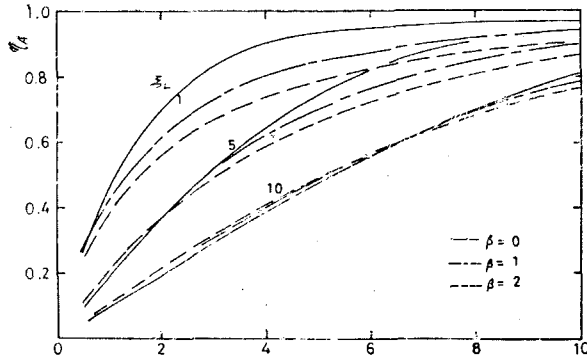


Fig. 10. Effect of  $\beta$  on  $\eta_A$

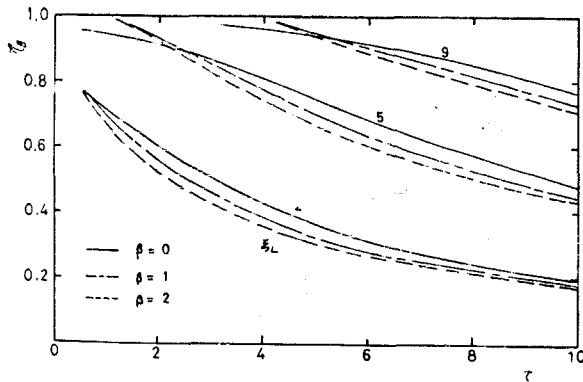


Fig. 11. Effect of  $\beta$  on  $\eta_B$

perature,  $T_0$ , is heated by a fluid (air in the present case) which enters at a constant, higher temperature,  $T_i$ . The temperature-time history of the several point is recorded during heating process.

The experimental apparatus and its dimensions are shown schematically in Fig. 12 and Table 1, respectively.

(1) The hollow cylinder made of carbon steel is used for heat storage medium and outer wall is insulated by glasswool and styroform.

(2) The air is supplied by a small sirocco fan capable of providing  $0.2 \text{ m}^3/\text{min}$  at 10 mmAq. Inlet power of 100 V-200 W electric

Table 1. Dimension of Heat Storage Medium

Type	$D(\text{m})$	$d(\text{m})$	$\epsilon$	$L(\text{m})$	$L(\text{m})$	Thermocouple
A	$3.06 \times 10^{-2}$	$1.06 \times 10^{-2}$	0.12	1	0.25	Fe-Const.
B	$1.73 \times 10^{-2}$	$0.93 \times 10^{-2}$	0.29	1	0.25	Cu-Const.

Table 2. Thermal Properties Used in Calculation

Substance	$c_p$ ( $\text{J}/\text{m}^3\text{K}$ )	$k$ ( $\text{W}/\text{mK}$ )	$\alpha$ ( $\text{m}^2/\text{s}$ )	$\alpha$ ( $\text{m}^2/\text{s}$ )	Pr
air (at 50C)	$1.103 \times 10^3$	0.028	—	$1.80 \times 10^{-5}$	0.70
steel (0.5% C)	$3.642 \times 10^6$	54	$1.48 \times 10^{-5}$	—	—

heating coil is controlled by thermostat and voltage controller for the purpose of obtaining the required temperature. The temperature of the supplied air is maintained at  $90^\circ\text{C}$  while room temperature ( $10^\circ\text{C}$ - $20^\circ\text{C}$ ) is regarded as initial temperature  $T_0$ .

(3) The temperature in the system are measured by 13 thermocouples which were made of iron constantan and copper-constantan. These are installed in fluid passage and inner wall of storage medium with equidistance as shown in Fig. 1. On the other hand, to examine the effect of radial direction conduction, three thermocouples are butted on the outer surface of the storage medium.

The thermocouple output (emf) is recorded by a 10-pen electric recorder and a digital thermometer. These instrument can read potentials within 0.01 mV. The experimental error of the temperature measuring system determined by precise potentiometer is presumed to be within  $1^\circ\text{C}$ .

(4) The air velocity is measured by a portable hot wire anemometer at twelve points and its arithmetic average was used.

Some comparisons of experimental re-

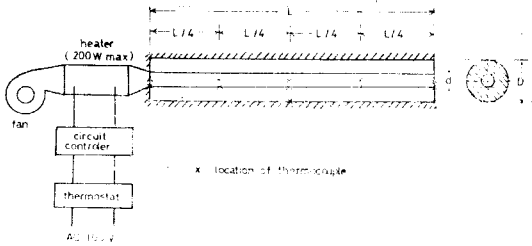


Fig. 12. Schematic diagram of experimental set up

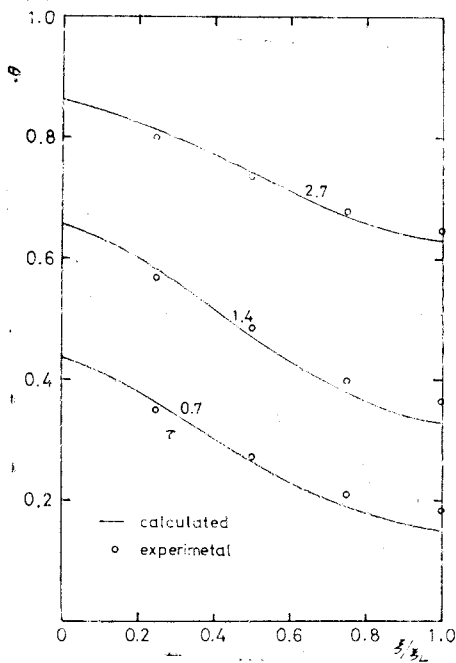


Fig. 13. Comparison of calculated value with experimental results (Type A,  $u=5\text{m/s}$ ,  $\beta=0.13$ )

sults with the calculated values of the governing equations are shown in Figs. 13 and 14. Thermal properties of air and steel which were used in calculation of experimental results are presented in Table 2. The temperature correction due to the radial direction was applied and the effect was small enough to see the general trend of the temperature history.

#### 4. RESULTS AND DISCUSSION

The solution of the nondimensionalized

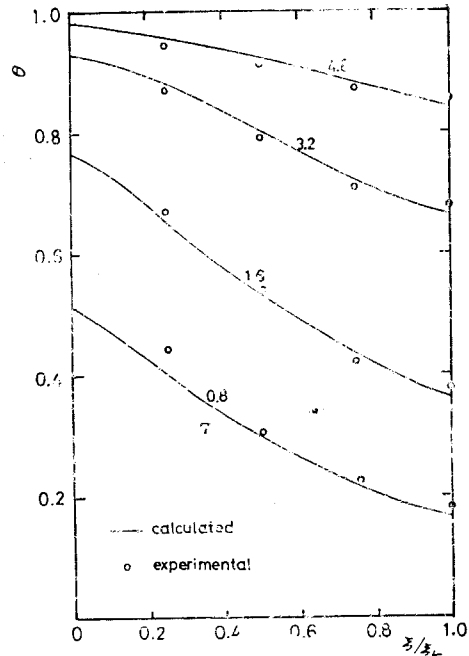


Fig. 14. Comparison of calculated value with experimental results (Type B,  $u=12\text{m/s}$ ,  $\beta=0.02$ )

Fig. 11 Effect of  $\beta$  on  $\eta_{ts}$ .

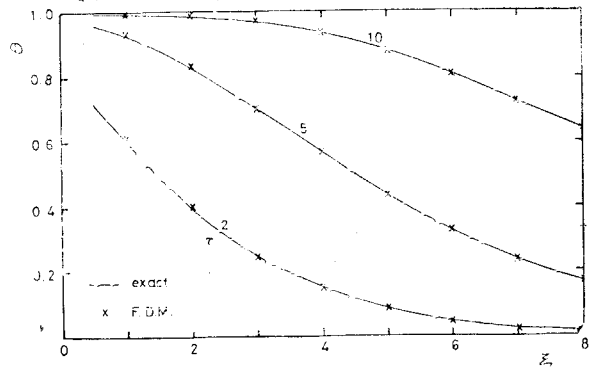


Fig. 15. Comparison of exact solution with the result of F. D. M.

governing equations were compared with the results of experiment in Figs. 13 and 14. Here, the experimentally measured temperatures are converted into the dimensionless ones. Acceptable agreements are observed through the comparison. The maximum deviation is less than  $2^\circ\text{C}$ .

It should be mentioned here that, al-

though the majority of practical problems may require finite difference methods to obtain detailed answer analytical methods are still important. In setting up a complex problem using finite differences, limiting cases are often have analytical solutions that can be used for comparison to the numerical results.

In this problem, the exact solution of the simultaneous partial differential equations (6) and (7) can be obtained in special case of  $\beta=0$  by means of Laplace transformation technique.<sup>8)</sup> The solutions are found to be

$$\nu = e^{-\xi} \left[ e^{-\tau} I_0(2\sqrt{\xi\tau}) + \int_0^{\tau} e^{-z} I_0(2\sqrt{\xi z}) dz \right] \quad (16)$$

$$\theta = e^{-\xi} \int_0^{\tau} e^{-z} I_0(2\sqrt{\xi z}) dz \quad (17)$$

The integrated values of the modified Bessel function of order zero are calculated by means of numerical quadrature and compared with the resultant values of finite difference method (Fig. 15). Reasonably good agreement was also found for  $\xi \geq 0.5$ .

It is disclosed from the study that:

(1) For the higher value of  $\beta$ , temperature-location diagram shows the tendency of uniform distribution, i.e., temperature of the inlet side of the system descends as  $\beta$  has higher value while temperature of the outlet side shows ascending tendency. (Figs. 6 and 7) Effects of  $\beta$  on efficiencies may be also detected in Figs. 10 and 11.

(2) Higher efficiency  $\eta_A$  was found for a system with higher value of  $\tau$  and/or lower value of  $\xi$  (Fig. 8).

(3) Contrary to (2), higher efficiency  $\eta_B$  was found for lower value of  $\tau$  and/or high-

er value of  $\xi$  (Fig. 9).

(4) The results of (2) and (3) suggest that there would be an optimum condition for the storage system. These results can be applied to the heat storage system which has considerable conduction effect along the axial direction, and they will give the temperature distributions, quantity of stored energy, and efficiencies if required.

### References

1. Jacob, Max, *Heat Transfer* Vol. 1, Wiley, 1957, Ch. 35.
2. Hughes, P.J., Klein, S.A., Close, D.J., "Packed Bed Thermal Storage Models for Solar Air Heating and Cooling Systems", *Trans. ASME, Series C. J. of Heat Transfer*, Vol. 98, No. 2, 1976, pp. 336-338.
3. Burch, D.M., Allen, R.W., Peave, B.A., "Transient Temperature Distribution within Porous Slabs Subjected to Sudden Transpiration Heating", *Trans. ASME, Series C. J. of Heat Transfer*, Vol. 98, No. 2 1976, pp. 221-225.
4. L6f, G.O.G., Hawley, R.W. "Unsteady State Heat Transfer Between Air and Loose Solids", *Ind. and Engr. Chem.*, Vol. 40, 1948, pp. 1061-1070.
5. Coppage, J.E., London, A.L., "Heat Transfer and Flow Friction Characteristics of Porous Media", *Chem. Engr. Prog.*, Vol. 52, No. 2, 1956, pp. 57-63.
6. Myers, G.E., *Analytical Methods in Conduction Heat Transfer*, McGraw Hill, 1971, Ch. 8.
7. Richtmyer, R.D., *Difference Methods for Initial Value Problems*, Interscience, 1967, Ch. 1.
8. Yang, W.J., Lee, C.P., *Dynamic Response of Solar Heat Storage Systems*, ASME Publication, 74-WA/HT-22, 1974.